



Stochastic Late Accretion to Earth, the Moon, and Mars

William F. Bottke, *et al.*
Science **330**, 1527 (2010);
DOI: 10.1126/science.1196874

This copy is for your personal, non-commercial use only.

If you wish to distribute this article to others, you can order high-quality copies for your colleagues, clients, or customers by [clicking here](#).

Permission to republish or repurpose articles or portions of articles can be obtained by following the guidelines [here](#).

The following resources related to this article are available online at www.sciencemag.org (this information is current as of March 6, 2012):

Updated information and services, including high-resolution figures, can be found in the online version of this article at:

<http://www.sciencemag.org/content/330/6010/1527.full.html>

This article **cites 37 articles**, 3 of which can be accessed free:

<http://www.sciencemag.org/content/330/6010/1527.full.html#ref-list-1>

This article appears in the following **subject collections**:

Planetary Science

http://www.sciencemag.org/cgi/collection/planet_sci

12. A. E. Dessler, P. Yang, Z. Zhang, *Geophys. Res. Lett.* **35**, L20704 (2008).
13. B. A. Wielicki *et al.*, *Bull. Am. Meteorol. Assoc.* **77**, 853 (1996).
14. The data used here are the SSF Edition 2.5 $1^\circ \times 1^\circ$ gridded, monthly averaged data. Edition 2.5 contains new Edition 3 calibration combined with Edition 2 algorithms and is available from <http://ceres.larc.nasa.gov>.
15. N. G. Loeb *et al.*, *J. Clim.* **20**, 575 (2007).
16. B. J. Soden *et al.*, *J. Clim.* **21**, 3504 (2008).
17. K. M. Shell, J. T. Kiehl, C. A. Shields, *J. Clim.* **21**, 2269 (2008).
18. A. Simmons, S. Uppala, D. Dee, S. Kobayashi, ERA-Interim: New ECMWF reanalysis products from 1989 onward (*ECMWF Newsletter* **110**, Winter 2006/2007). Data can be downloaded from www.ecmwf.int/products/data.
19. M. J. Suarez *et al.*, The GEOS-5 Data Assimilation System—documentation of versions 5.0.1, 5.1.0, and 5.2.0, NASA/TM-2008-104606, Vol. 27, 2008. Data can be downloaded from <http://disc.sci.gsfc.nasa.gov>.
20. A. E. Dessler *et al.*, *J. Geophys. Res.* **113**, D17102 (2008).
21. L. Moy *et al.*, *J. Geophys. Res.* **115**, D15110 (2010).
22. B. J. Soden, R. Bennartz, *J. Geophys. Res.* **113**, D20107 (2008).
23. C. A. Smith, P. D. Sardeshmukh, *Int. J. Climatol.* **20**, 1543 (2000).
24. K. E. Trenberth, J. T. Fasullo, C. O'Dell, T. Wong, *Geophys. Res. Lett.* **37**, L03702 (2010).
25. D. M. Murphy, *Geophys. Res. Lett.* **37**, L09704 (2010).
26. M. H. Zhang, J. J. Hack, J. T. Kiehl, R. D. Cess, *J. Geophys. Res.* **99**, 5525 (1994).
27. R. W. Spencer, W. D. Braswell, *J. Geophys. Res.* **115**, D16109 (2010).
28. I. M. Held, B. J. Soden, *Annu. Rev. Energy Environ.* **25**, 441 (2000).
29. K. Minschwaner, A. E. Dessler, *J. Clim.* **17**, 1272 (2004).
30. A. E. Dessler, S. C. Sherwood, *Science* **323**, 1020 (2009).
31. G. A. Meehl *et al.*, *Bull. Am. Meteorol. Soc.* **88**, 1383 (2007).
32. P. Huybers, *J. Clim.* **23**, 3009 (2010).
33. E. S. Chung, B. J. Soden, B. J. Sohn, *Geophys. Res. Lett.* **37**, L10703 (2010).
34. M. Zelinka, D. L. Hartmann, *J. Geophys. Res.* **115**, D16117 (2010).
35. I thank the CERES, MERRA, and ECMWF groups for producing the data used in this paper. Support for this work came from NASA grant NNX08AR27G to Texas A&M University. I also acknowledge useful contributions from N. Loeb, M. Bosilovich, J.-J. Morcrette, M. Zelinka, P. Stackhouse, T. Wong, J. Fasullo, P. Yang, and G. North. Finally, I acknowledge the modeling groups, the Program for Climate Model Diagnosis and Intercomparison, and the WCRP's Working Group on Coupled Modeling for their roles in making available the WCRP CMIP3 multimodel data set. Support of this data set is provided by the U.S. Department of Energy Office of Science.

19 May 2010; accepted 9 November 2010
10.1126/science.1192546

Stochastic Late Accretion to Earth, the Moon, and Mars

William F. Bottke,^{1*} Richard J. Walker,² James M. D. Day,^{2,3} David Nesvorný,¹ Linda Elkins-Tanton⁴

Core formation should have stripped the terrestrial, lunar, and martian mantles of highly siderophile elements (HSEs). Instead, each world has disparate, yet elevated HSE abundances. Late accretion may offer a solution, provided that $\geq 0.5\%$ Earth masses of broadly chondritic planetesimals reach Earth's mantle and that ~ 10 and ~ 1200 times less mass goes to Mars and the Moon, respectively. We show that leftover planetesimal populations dominated by massive projectiles can explain these additions, with our inferred size distribution matching those derived from the inner asteroid belt, ancient martian impact basins, and planetary accretion models. The largest late terrestrial impactors, at 2500 to 3000 kilometers in diameter, potentially modified Earth's obliquity by $\sim 10^\circ$, whereas those for the Moon, at ~ 250 to 300 kilometers, may have delivered water to its mantle.

Highly siderophile elements (HSEs: Re, Os, Ir, Ru, Pt, Rh, Pd, Au) have low-pressure metal-silicate partition coefficients that are extremely high ($>10^4$) (1). Hence, a common assumption has been that the silicate portions of rocky planetary bodies with metallic cores are effectively stripped of HSEs immediately after primary accretion and final core segregation (2). Accordingly, the “giant impact” on Earth that formed the Moon 60_{-10}^{+90} million years (My) after formation of the earliest solids should have cleansed HSEs from the mantles of both worlds (3–5).

However, studies of mantle-derived terrestrial peridotites (olivine-rich rocks that dominate Earth's upper mantle) have shown that, not only are HSE abundances in Earth's mantle much higher than expected (at $\sim 0.008 \times$ CI-chondrite

meteorites), but their HSE proportions are also approximately the same as chondritic meteorites (Fig. 1) (6). Although we have no direct samples of martian or lunar mantle rocks, studies of HSE and Os isotopes in derivative mantle melts sug-

gest roughly equivalent absolute abundances in the martian mantle (7, 8), but much lower abundances in the lunar mantle ($\leq 0.0004 \times$ CI-chondrite) (9–11), with HSEs in chondritic relative proportions for both bodies (Fig. 1) (7, 10).

Although different scenarios have been proposed to produce the relatively high absolute and chondritic relative abundances of HSEs in planetary mantles (12), perhaps the most straightforward process is delivery from continued planetesimal accretion after the last core-formation event, with the materials mixed into the mantle by convection (13). Such events would represent a natural continuum from a planet-formation perspective, with the Mars-sized projectile that produced the giant impact representing the largest component of the leftover planetesimal population that continued to bombard the planets until surviving projectiles were depleted by collisional and dynamical processes (14).

We used the estimated collective distribution of HSEs in the terrestrial, martian, and lunar mantles to test whether their abundances were set by late accretion. For Earth, late accretion of $\sim 2.0 \times 10^{22}$ kg of material with bulk chondritic

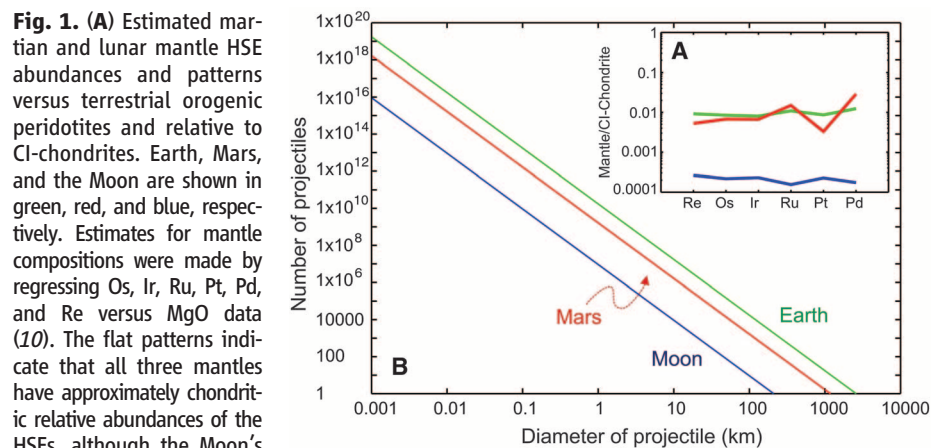


Fig. 1. (A) Estimated martian and lunar mantle HSE abundances and patterns versus terrestrial orogenic peridotites and relative to CI-chondrites. Earth, Mars, and the Moon are shown in green, red, and blue, respectively. Estimates for mantle compositions were made by regressing Os, Ir, Ru, Pt, Pd, and Re versus MgO data (10). The flat patterns indicate that all three mantles have approximately chondritic relative abundances of the HSEs, although the Moon's mantle abundances are >20

times less than those of Earth. (B) Minimum number and sizes of late accretion chondritic projectiles needed to deliver the estimated abundances of HSEs to the mantles of the Moon, Mars, and Earth, assuming 100% accretion efficiency. These values are lower limits in terms of delivered mass because the process is unlikely to be 100% efficient.

¹Southwest Research Institute and NASA Lunar Science Institute, 1050 Walnut Street, Suite 400, Boulder, CO 80302, USA. ²Department of Geology, University of Maryland, College Park, MD 20742, USA. ³Geosciences Research Division, Scripps Institution of Oceanography, La Jolla, CA 92093, USA. ⁴Massachusetts Institute of Technology, Cambridge, MA 02139, USA.

*To whom correspondence should be addressed. E-mail: bottke@boulder.swri.edu

composition is required to reproduce measured mantle peridotite compositions (15), assuming even distribution of the HSEs throughout the mantle (12). This quantity of mass does not violate Earth-Moon isotopic constraints, such as for oxygen, examined to date (16, 17). If martian mantle abundances of the HSEs are similar to the terrestrial mantle (we assume that HSE abundances are $0.7 \times$ terrestrial mantle abundances), late accretion of $\sim 2.0 \times 10^{21}$ kg of material would be necessary for that planet (15). A proportionally much lower amount of mass ($\sim 1.7 \times 10^{19}$ kg) is needed for the Moon (10, 15), assuming that lunar mantle abundances are $\leq 0.05 \times$ terrestrial mantle abundances and the lunar core is only $\sim 4\%$ of the Moon's mass (11). These mass estimates yield Earth/Mars and Earth/Moon input mass ratios of ~ 10 and ~ 1200 , respectively.

The high Earth/Moon input mass ratio is curious on several levels. For example, the Earth/Moon impact number flux ratio for both late-accreting planetesimals and present-day near-Earth objects is ~ 20 , with this value being a reflection of their different gravitational cross-sectional areas (14, 18, 19). Micrometeorites, many of which achieve nearly circular orbits with Earth and the Moon via nongravitational forces

before impact, only reach an impact number flux value of ~ 50 , with the increase coming from gravitational focusing by Earth (19). Thus, it seems unlikely that small, numerous projectiles could ever achieve mass input ratios close to 1200 in the aftermath of the Moon-forming event when most leftover planetesimals, asteroids, or comets in the inner solar system were dynamically excited (14).

It is possible to lower the Earth/Moon input mass ratio by assuming that the Moon retained less impactor material than did Earth or Mars. Numerical simulations show that ~ 60 and $\sim 15\%$ of the mass of stony and water-ice impactors residing in the inner solar system, respectively, are retained on the Moon after an impact (20). Water-ice cannot carry HSEs, so a reasonable retention factor for standard cometary ice-rock compositions is $\sim 30\%$ (21). This could conceivably lower the ratio to between 400 and 700. However, if projectiles delivering HSEs were denser and/or volatile-poor, such as differentiated or iron-rich planetesimals, more mass might be retained, moving the range to 700 to 1200, or higher.

An additional constraint is that most HSEs had to be delivered to the lunar, terrestrial, and martian mantles within tens of million years of

core-formation termination. The lunar crust, which formed 4.42 to 4.46 billion years ago (Ga) or possibly earlier, is essentially intact and has only been modestly contaminated by extra-lunar materials (5, 10–12, 22). Thus, most of the HSEs in the terrestrial and lunar mantles arrived before this time. Late-arriving projectiles could potentially modify Earth's HSE budget, because their mass could reach the mantle via plate tectonic processes, but the net mass delivered would be limited because some fraction would unavoidably end up on the Moon where it is not observed. For Mars, Nd-Os isotopic correlations indicate that mantle reservoirs were isolated within ~ 20 My of differentiation (7). This implies that most HSEs were delivered by leftover debris from terrestrial planet accretion, which was probably dominated by stony, iron, and/or differentiated planetesimals, rather than comets (6, 23). Accordingly, the Earth/Moon input mass ratio is probably >700 .

By combining these constraints within a Monte Carlo code, we explored whether any plausible late accretion size distributions were capable of delivering the estimated abundances of mass and, consequently, HSEs to Earth, Mars, and the Moon (24). For Earth and the Moon, whose origins and last core-formation events are linked together in time, and assuming a projectile size distribution $dN \propto D^{-q}dD$ (where dN is the number of objects of diameter D within a bin dD , and q is the differential power-law index), our best results came from simulations where $q < 2$ and few projectiles between 200 and 4000 km diameter hit the Moon (Fig. 2). This combination allowed large impactors to produce profound differences in delivered mass and HSEs to the mantles of the worlds they struck.

Although the precise projectile size range needed to match Earth/Moon constraints is unknown, modeling work does set limits (16). In the absence of plate tectonics, late accretion impactors needed to be large enough to breach early planetary lithospheres, create local magma ponds from their impact energy, and then efficiently mix into the mantle, but not so large that their impact-fragmented core coalesced with the planet's core. Assuming an end-member case (25), where a world is still in a magma ocean phase, the iron core of a differentiated projectile, assumed here to be about half the projectile's diameter, will become emulsified into the mantle if it is smaller than the depth of the magma ocean. For Earth, Mars, and the Moon, this criterion roughly limits HSE delivery among differentiated projectiles to diameters <2000 to 4000 km (26), <1000 to 3000 km (27), and <1000 km (5), respectively. Projectiles striking after this phase need to punch through the body's newly formed lithosphere, and some will not make it. For those that do, fragmentation experienced en route to the mantle may break down the core into smaller pieces more suitable for emulsification (16).

For projectiles larger than 10% of the diameter of the target world, HSE delivery is mainly

Fig. 2. Results from a Monte Carlo code simulation showing the differential power-law index q of the SFDs most likely to deliver the appropriate quantity of late accretion projectiles to Earth and the Moon (24). The colored lines correspond to the maximum projectile size that could potentially strike the worlds (D_{\max}). Low q values correspond to shallow size distributions where most of the mass of the colliding population is in the largest projectiles.

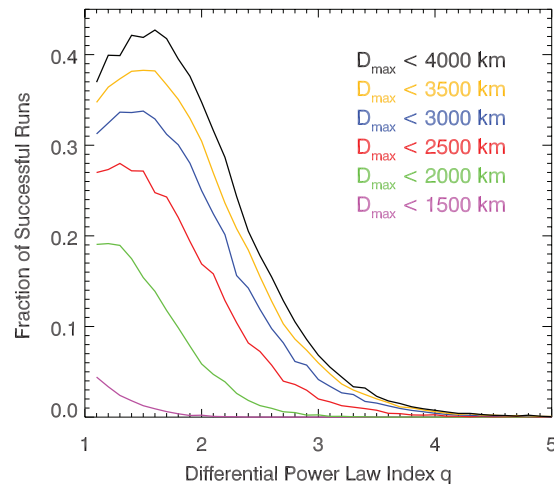
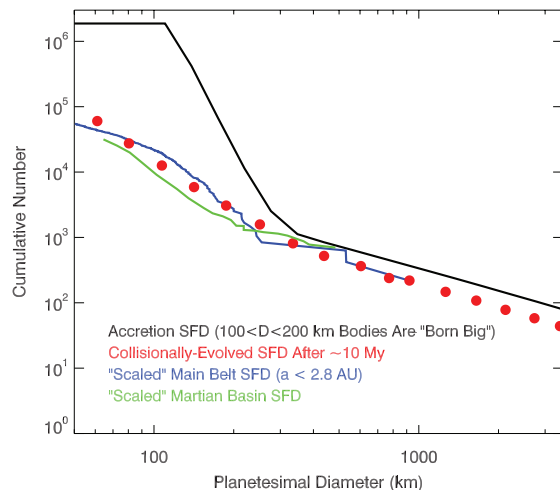


Fig. 3. SFDs of planetesimal populations at different evolution stages compared with data from the asteroid belt and ancient martian basins. The black curve represents an accretion SFD at 1 AU with planetesimals born big between $D \sim 100$ and 200 km. The shallow branch of the SFD for $D > 250$ km was produced by runaway growth and has $q \sim 2.2$. The red dots show that ~ 10 My of collisional evolution among the accretion SFD does not affect the slope of the $D > 250$ -km objects. The blue curve shows a scaled version of the inner and central main belt SFDs, defined as asteroids with semimajor axis $a < 2.8$ AU. The green line shows the estimated projectile SFD computed from martian impact basins.



controlled by the physics of so-called “hit and almost run” collisions (28), in which most of the projectile’s core (and HSEs) plows through the target’s mantle and emerges on the other side in a highly fragmented state. The debris then evolves into a long spiral-armlike structure that proceeds to rain down across the target over many hours. Thus, these events would allow massive impactors to stochastically deliver large quantities of HSEs, but in a manner akin to small-body accretion that optimizes emulsification into the upper mantle (16). If the largest terrestrial late accretion events were of this nature, several ongoing conundrums may be explained, including why mantle peridotites in Earth’s early rock record have surprisingly similar, although not necessarily uniform HSE abundances (29, 30) and how the iron in the projectile’s core became oxidized (9, 31).

Assuming the late accretion size distribution hitting Earth, the Moon, and Mars had $q \sim 2$, the best-case Monte Carlo results yield mean and median diameters of the largest Earth and Moon impactors of 2500 to 3000 km and 250 to 300 km, respectively. For Mars, whose formation, differentiation, and evolution are not linked in time to the Earth-Moon system, we developed an alternative Monte Carlo code. Choosing random projectiles from a size distribution and terminating each run when the net accreted mass exceeded 2.6×10^{21} kg, we found that the largest mean and median projectiles to strike Mars were 1500 to 1800 km in diameter. For impact velocities of ~ 10 km/s, this range matches the computed projectile size needed to create the proposed 10,600-by-8500-km Borealis basin (32).

Our preferred late accretion populations (those with $q \sim 2$) appear to be consistent with results from numerical simulations in which submeter objects in the protoplanetary disk are concentrated by turbulence into gravitationally bound clumps that collapse to form $D \sim 100$ -km planetesimals (33–35). Because the new planetesimals are born big, they avoid the many survival problems faced by $D = 0.001$ -km to multikilometer planetesimals, namely gas drag driving them into the Sun or disruption via impacts from numerous smaller objects embedded in the gas disk.

We produced an accretion size distribution closely resembling runs from our previous numerical experiments (33, 36), where 1.6 Earth masses of material were placed into $D = 2$ -m objects coupled to a gas disk near 1 astronomical unit (AU) and left to evolve for ~ 2 My (Fig. 3). Here, once sufficient numbers of $D \sim 100$ -km planetesimals were created, a subset of the population underwent runaway growth and developed into a shallow $q \sim 2$ size distribution that stretches from $D > 200$ - to 300-km planetesimals all the way to planetary embryo sizes. Next, we assumed the planetesimals were dynamically excited enough by gravitational interactions with planetary embryos to induce collisional evolution (Fig. 3). The objects were given new collision probabilities and impact velocities based on

numerical simulations that tracked how planetary embryos near 1 AU affect a background planetesimal population (37, 38). After ~ 10 My, we found that many $D \sim 100$ -km bodies were smashed into rubble. Larger planetesimals, however, were harder to disrupt, with the bodies finding increasing protection via their own gravity. Apparently, once a planetesimal size distribution develops a shallow branch among large objects, it is there to stay.

Observational evidence also exists to support the idea that large planetesimals in regions adjacent to the 1-AU zone had $q \sim 2$ size distributions. In the inner and central asteroid belts (with semimajor axis < 2.8 AU), the only known asteroids beyond $D > 250$ km are Ceres, Pallas, and Vesta, with $D = 975, 544,$ and 530 km, respectively (Fig. 3) (39). A power-law slope determined for asteroids between $D = 250$ and 975 km yields $q \sim 1.8$, the same as those favored in Fig. 2. Notably, the outer asteroid belt follows a power-law size-frequency distribution (SFD) in the range $100 < D < 400$ km and has no shallow branch at large sizes. Although the absence of $D > 400$ -km objects may be a by-product of small number statistics and/or collisional/dynamical evolution, the other shape differences between the inner and outer main-belt size distributions imply that planetesimal-formation mechanisms change as one approaches the so-called snowline and/or that the outer asteroid belt has been contaminated by outer solar system planetesimals captured during giant planet migration (40).

Additional observational evidence comes from ancient martian impact basins, defined as $D > 300$ -km diameter craters, that formed during the earliest bombardment phases of the solar system. Their ages are unknown, though numerical simulations suggest that the oldest impact basins were produced by leftover planetesimals in the terrestrial planet region (14), whereas the youngest probably came from colliding comets and asteroids liberated from stable reservoirs during the last substantial giant planet migration event ~ 4 Ga (40). Using populations of buried and visible basins on Mars that have been previously cataloged (41), scaling relations for complex craters from (42), and impact velocities derived from (14, 18), we transformed those basins not in saturation equilibrium (namely those with $D = 700$ to 2000 km) into a projectile size distribution (Fig. 3). As before, the impactors with $D > 200$ to 300 km have $q \sim 1.8$.

Our inferred late accretion populations may have substantially modified Earth’s rotational angular momentum vector, perhaps enough to violate constraints. To test this, we tracked the effects of inelastic collisions between Earth and suites of projectiles computed from the most favorable cases shown in Fig. 2. We found that for a range of reasonable post-giant impact values (43), Earth’s rotational angular momentum changed by ~ 1 to 4%. On average, more than half of the input angular momentum was

delivered by the largest projectile in the suite, which tended to be between 2500 and 3500 km diameter. Moreover, in at least 50% of these trial cases, Earth’s obliquity was altered by 5° to 15° .

Such an obliquity change could help to explain the Moon’s orbital inclination, but only if the projectiles struck soon after the Moon-forming event. The Moon is believed to have formed in Earth’s equatorial plane, but shortly thereafter it obtained a primordial orbital inclination value of $\sim 10^\circ$ (3). Modeling work suggests that this value was produced by gravitational interactions between the Moon and the protolunar disk (44). If the protolunar disk was too short-lived to produce the full inclination, however, late terrestrial impacts could have made up the difference by altering Earth’s obliquity by up to $\sim 10^\circ$. To work, delivered HSEs could not be sequestered to Earth’s core, no easy task given the dynamic, high-temperature environment of Earth at this time, and the largest impactors would need to hit before Earth’s tides pushed the Moon beyond ~ 20 Earth radii from Earth (3). Note that the estimated interval for the latter, on the order of ~ 1 My, is short compared with numerical computations of late accretion time scales.

The Moon’s interior was once thought to be largely dry, with bulk water estimates of less than 1 part per billion (ppb) (45). Recent sample measurements, however, suggest that the water content in the lunar mantle is between 200 and several thousand ppb (or more) (45, 46). If true, it is possible that the same projectile that delivered most of the Moon’s HSEs may have also provided it with water. Assuming that our inferred $D = 250$ - to 300 -km lunar projectile could reach and mix itself into a spherical shell that is 100 to 500 km deep within the Moon and that the projectile had a minimum bulk water content of 0.05 to 0.2 weight percent (wt %) (47, 48), we estimate that 400 to 3000 ppb water could be delivered to the lunar interior by late accretion. Thus, late accretion provides an alternative explanation in case lunar mantle water cannot migrate from the post-giant impact Earth to a growing Moon through a hot and largely vaporized protolunar disk (3).

References and Notes

1. A. Borisov, H. Palme, B. Spettel, *Geochim. Cosmochim. Acta* **58**, 705 (1994).
2. J. H. Jones, M. J. Drake, *Nature* **323**, 470 (1986).
3. R. M. Canup, *Annu. Rev. Astron. Astrophys.* **42**, 441 (2004).
4. M. Touboul, T. Kleine, B. Bourdon, H. Palme, R. Wieler, *Nature* **450**, 1206 (2007).
5. P. H. Warren, in *Meteorites, Comets and Planets: Treatise on Geochemistry*, A. M. Davis, H. D. Holland, K. K. Turekian, Ed. (Elsevier, Amsterdam, 2005), vol. 1, pp. 559–599.
6. H. Becker et al., *Geochim. Cosmochim. Acta* **70**, 4528 (2006).
7. A. D. Brandon, R. J. Walker, J. W. Morgan, G. G. Goles, *Geochim. Cosmochim. Acta* **64**, 4083 (2000).
8. J. H. Jones, C. R. Neal, J. C. Ely, *Chem. Geol.* **196**, 21 (2003).
9. R. J. Walker, M. F. Horan, C. K. Shearer, J. J. Papike, *Earth Planet. Sci. Lett.* **224**, 399 (2004).
10. J. M. D. Day, D. G. Pearson, L. A. Taylor, *Science* **315**, 217 (2007).

11. J. M. D. Day, R. J. Walker, O. B. James, I. S. Puchtel, *Earth Planet. Sci. Lett.* **289**, 595 (2010).
12. R. J. Walker, *Chem. Erde* **69**, 101 (2009).
13. C.-L. Chou, *Proc. Lunar Planet. Sci. Conf.* **9**, 219 (1978).
14. W. F. Bottke, H. F. Levison, D. Nesvorný, L. Dones, *Icarus* **190**, 203 (2007).
15. By taking the ratio of Os concentration in the primitive upper mantle (~3.3 ppb) against the average concentration of all three chondrite groups weighted equally (~660 ppb) (12), we estimate that the terrestrial mass addition fraction is 0.005. Assuming the mass of Earth's mantle is 4.0×10^{24} kg, the terrestrial mass addition requirement is 2.0×10^{22} kg. A similar calculation can be made for Mars. If HSEs in the martian mantle are $0.7 \times$ the terrestrial concentration [for example, 2.4 ppb Os; consistent with the current database for shergottites (8)], and the martian mantle comprises ~80% of the mass of the planet (5.1×10^{23} kg), the martian mass addition requirement is $\sim 2.0 \times 10^{21}$ kg. This yields a ratio for terrestrial/martian additions of 10. For the Moon, assuming HSE abundances in the lunar mantle are ≤ 20 times lower than in the terrestrial mantle (9, 10), we obtain a maximum Os concentration of 0.16 ppb. Assuming the mass of the lunar mantle is 6.9×10^{22} kg and the same average chondritic concentration for the impactors, we obtain a lunar mass addition requirement of 1.7×10^{19} kg. This yields a ratio for terrestrial/lunar additions of 1200.
16. T. W. Dahl, D. J. Stevenson, *Earth Planet. Sci. Lett.* **295**, 177 (2010).
17. Late accretion of this magnitude would have had a modest effect on the W isotopic composition of Earth. The amount of impactor(s) mass envisioned to add the HSEs to the mantle would also add ~10% of the total W present in the silicate Earth (assuming that ~10% of the W presently resides in the silicate portion of Earth and that the late accretion impactor made up ~1% of the mass of the mantle). The ϵ_W value of bulk-silicate Earth, defined as a part in 10,000 deviation of $^{182}\text{W}/^{184}\text{W}$ from the terrestrial ratio, is 0. If the bulk impactor had an ϵ_W value of -2.0 (chondritic) at the time of impact, as seems likely, mass balance requires that the ϵ_W value of the silicate Earth before impact was $\sim +0.2$. If the silicate Earth and Moon had the same ϵ_W value and W concentrations at the time of the Moon-forming giant impact event (16), the Moon should have a slightly higher ϵ_W value after the proposed late accretion event. The current best estimate for the ϵ_W value for the Moon is $+0.09 \pm 0.10$ (2 σ) (4). Within uncertainties, this value is ambiguously identical to both the present terrestrial value and the projected pre-late accretion impact Earth.
18. W. F. Bottke *et al.*, *Icarus* **156**, 399 (2002).
19. D. Nesvorný *et al.*, *Astrophys. J.* **713**, 816 (2010).
20. N. A. Artemieva, V. V. Shuvalov, *Sol. Syst. Res.* **42**, 329 (2008).
21. We calculated an average projectile retention factor of ~30% for planetesimals composed of 50-50 ice/rock mixtures by splitting the difference between the data in (20) for stony and water-ice projectiles striking the Moon at 18 and 25 km/s, respectively. We exclude nearly isotropic comets from our analysis because they are extremely unlikely to hit Earth and the Moon in the interval between the Moon-forming impact and the solidification of the lunar crust.
22. I. S. Puchtel, R. J. Walker, O. B. James, D. A. Kring, *Geochim. Cosmochim. Acta* **72**, 3022 (2008).
23. A. N. Halliday, in *Meteorites, Comets and Planets: Treatise on Geochemistry*, A. M. Davis, H. D. Holland, K. K. Turekian, Ed. (Elsevier, Amsterdam, 2005), vol. 1, pp. 509–557.
24. Projectiles were randomly selected from a size distribution $dN \propto D^{-q}dD$. The range of D was set to 200 to 4000 km; this was designed to provide some flexibility in case the largest projectiles deliver only ~80 to 90% of their HSEs to the mantle. A successful run had an Earth/Moon mass ratio >700 with the accreted mass on Earth set to $>2.0 \times 10^{22}$ kg. The Earth/Moon impact number flux ratio was set to 20 (14, 18, 19). The sizes of the largest impactors, as well as the number of objects hitting each world within a given run were treated as variables.
25. D. C. Rubie, H. J. Melosh, J. E. Reid, C. Liebske, K. Righter, *Earth Planet. Sci. Lett.* **205**, 239 (2003).
26. D. C. Rubie, C. K. Gessmann, D. J. Frost, *Nature* **429**, 58 (2004).
27. L. E. Borg, D. S. Draper, *Meteorit. Planet. Sci.* **38**, 1713 (2003).
28. E. Asphaug, *Chem. Erde* **70**, 199 (2010).
29. V. C. Bennett, A. P. Nutman, T. M. Esat, *Geochim. Cosmochim. Acta* **66**, 2615 (2002).
30. W. D. Maier *et al.*, *Nature* **460**, 620 (2009).
31. If the proposed late accretion impactor(s) added to Earth was differentiated and contained substantial metallic iron, our model requires that the metal eventually oxidized and/or remained forever isolated from the core. This is because metal removal to the core would also lead to removal of the majority of the impactor's HSE contribution. The issue of relict metal, resulting from such an event, can be resolved via oxidation. Because the amount of metal added to the mantle by our late accretion model would comprise only ~0.3% of the total mass of the mantle (assuming that 30% of the mass of the impactor was metal and that the mass of the impactor was 1% of the mass of the mantle), it could have been oxidized by reaction with ferric iron in the early mantle. This would imply that the $\text{Fe}^{3+}/\Sigma\text{Fe}$ ratio (where ΣFe is total Fe) of the mantle before the impact was ~0.15, rather than the present estimate of ~0.1, which is well within the range of ferrous/ferric ratios possible for the early Earth, based on chondritic comparisons.
32. M. M. Marinova, O. Aharonson, E. Asphaug, *Nature* **453**, 1216 (2008).
33. A. Morbidelli, W. F. Bottke, D. Nesvorný, H. F. Levison, *Icarus* **204**, 558 (2009).
34. A. Johansen *et al.*, *Nature* **448**, 1022 (2007).
35. J. N. Cuzzi, R. C. Hogan, W. F. Bottke, *Icarus* **208**, 518 (2010).
36. See figure 6, A and B, of (33). A detailed discussion of the code and approximations used in this simulation can be found in (33).
37. W. F. Bottke, D. Nesvorný, R. E. Grimm, A. Morbidelli, D. P. O'Brien, *Nature* **439**, 821 (2006).
38. The intrinsic collision probabilities (P_i) and impact velocities (V) of stony planetesimals striking one another near 1 AU were computed from the numerical runs described in (37). We estimate that at ~1 AU, $P_i = 60 \times 10^{-18} \text{ km}^{-2} \text{ yr}^{-1}$ and $V = 11 \text{ km/s}$.
39. P. Farinella, D. R. Davis, *Icarus* **97**, 111 (1992).
40. H. F. Levison *et al.*, *Nature* **460**, 364 (2009).
41. H. V. Frey, *J. Geophys. Res. Planets* **111**, E08591 (2006).
42. K. A. Holsapple, *Annu. Rev. Earth Planet. Sci.* **21**, 333 (1993).
43. The primordial Earth was assumed to have a spin period between 6 and 8 hours. The late accretion projectiles were assumed to hit at random locations with isotropic impact angles and impact velocities between 12 and 18 km/s.
44. W. R. Ward, R. M. Canup, *Nature* **403**, 741 (2000).
45. F. M. McCubbin *et al.*, *Proc. Natl. Acad. Sci. U.S.A.* **107**, 11223 (2010).
46. Z. D. Sharp, C. K. Shearer, K. D. McKeegan, J. D. Barnes, Y. Q. Wang, *Science* **329**, 1050 (2010); 10.1126/science.1192606.
47. F. Robert, *Space Sci. Rev.* **106**, 87 (2003).
48. We chose ordinary and enstatite chondrites from (47) because they probably resemble the nature of planetesimals in the terrestrial planet region (6, 23). It is unclear, however, whether the measured water is consistent with the overall reduced nature of the rocks. The water may be from terrestrial weathering, though there are arguments against this (47). Regardless, the cited water quantities (0.05 to 0.2 wt %) are much lower than those in carbonaceous chondrite meteorites (1 to 10 wt %) (47). It is entirely possible that a $D = 250$ - to 300-km planetesimal striking the Moon during late accretion would have such bulk quantities of water.
49. We thank A. Barr, R. Canup, R. Citron, L. Dones, H. Levison, J. Jones, H. Nekvasil, A. Morbidelli, D. Minton, S. Mojzsis, G. J. Taylor, and D. Vokouhlicky for many useful discussions and two anonymous reviewers for constructive reviews. W.F.B.'s and D.N.'s participation was supported by NASA's Lunar Science Institute through a grant to the Center for Lunar Origin and Evolution at the Southwest Research Institute in Boulder, Colorado. R.J.W.'s and J.M.D.'s work was supported by NASA's Lunar Science Institute through contract NNA09DB33A to the Center for Lunar Science and Exploration at the Lunar and Planetary Institute in Houston, Texas, and the NASA Astrobiology Program through grant NNG04G49A to the Goddard Center for Astrobiology in Greenbelt, Maryland.

24 August 2010; accepted 10 November 2010
10.1126/science.1196874

Thought for Food: Imagined Consumption Reduces Actual Consumption

Carey K. Morewedge,^{1*} Young Eun Huh,² Joachim Vosgerau²

The consumption of a food typically leads to a decrease in its subsequent intake through habituation—a decrease in one's responsiveness to the food and motivation to obtain it. We demonstrated that habituation to a food item can occur even when its consumption is merely imagined. Five experiments showed that people who repeatedly imagined eating a food (such as cheese) many times subsequently consumed less of the imagined food than did people who repeatedly imagined eating that food fewer times, imagined eating a different food (such as candy), or did not imagine eating a food. They did so because they desired to eat it less, not because they considered it less palatable. These results suggest that mental representation alone can engender habituation to a stimulus.

People believe that thinking about a desirable food or drug sensitizes one to it, increasing their hedonic response to the stimulus (1). Indeed, picturing oneself eating a delicious steak elicits an increase in salivation

and the desire to eat it (2), and imagining the sight or smell of a burning cigarette increases smokers' craving (3). The increased desirability of imagined stimuli seems to similarly affect behavior: Children have greater difficulty resisting